

Advances in Prevention of Thermal Runaway in Lithium-Ion Batteries

Rachel D. McKerracher,* Jorge Guzman-Guemez, Richard G. A. Wills, Suleiman M. Sharkh, and Denis Kramer

The prevention of thermal runaway (TR) in lithium-ion batteries is vital as the technology is pushed to its limit of power and energy delivery in applications such as electric vehicles. TR and the resulting fire and explosion have been responsible for several high-profile accidents and product recalls over the past decade. Herein, the causes of TR are described and novel preventative methods are examined, approaching the problem from different angles by altering the internal structure of the battery to undergo thermal shutdown or developing the battery and thermal management systems so that they can detect and prevent TR. Ultimately, a variety of different technologies is needed to address the emerging market of highly specialized lithium-ion batteries. Key innovations discussed include positive temperature coefficient (PTC) materials, self-healing polymer electrolytes, and hybrid liquid–solid-state electrolytes. Mist cooling achieves a highly uniform temperature inside the battery pack without the need for pumps to circulate a coolant. The development of battery management systems (BMSs) which model the internal temperature of the cell from real-time data and prevent the cell reaching a critical temperature is an essential area for further research.

1. Introduction

The last couple of decades have seen unprecedented demand for high-performance batteries for electric vehicles, aerial surveillance technology, and grid-scale energy storage. The European Council for Automotive R&D has set targets for automotive battery energy density of 800 Wh L^{-1} , with 350 Wh kg^{-1} specific energy and 3500 W kg^{-1} peak specific power.^[1] However, the

push toward ever higher energy and power densities increases the risk of dangerous accidental release of energy from the batteries.^[2] Although lithium-ion batteries have become safer in many ways since their invention, there remains the risk of fire and explosion caused by thermal runaway (TR). This is an exponential increase in temperature at a rate that cannot be dissipated quickly enough to the surroundings, caused by exothermic chemical decomposition of the materials inside the cells. The heat generated can propagate to other cells, causing a dangerous chain reaction where neighboring cells also begin to undergo TR. This can result in the entire battery pack being consumed in a fire or even exploding.

Most reported incidents of TR were caused by internal or external short circuits resulting from abuse of the cell or by sub-optimal cell design. For example, short circuits

resulting from the crash of a Tesla model X in China in 2017 caused the battery pack to catch fire. A famous example of a design issue is the recall of the Samsung Note 7 in 2016 due to an excessively thin separator which led to short circuits, causing several devices to explode.^[3]


The risks associated with TR have practical implications for how lithium-ion batteries can be transported, stored, and used. For example, lithium-ion batteries have caught fire in the hold of commercial aircraft,^[4] and there are now UN regulations regarding their safe transportation.^[5] Fires caused by lithium-ion battery failure onboard a ferry in 2019, in a parked Jaguar i-Pace in 2018, and other similar incidents have prompted requests for further improvement in lithium-ion battery testing standards to reflect real conditions of use.^[6]

All lithium-ion batteries must go through safety and abuse tests, based on those recommended by the Society of Automotive Engineers (SAE).^[7,8] These include mechanical, thermal, and electrical abuses, designed to create conditions that could lead to TR (Figure 1). It is essential to develop lithium-ion batteries that do not undergo TR, even when subjected to conditions of extreme abuse. The ideal design would prevent flow of electric current as soon as the internal cell temperature starts to increase close to the level that can cause TR, to prevent any risks of fire or damage to the cells.

This Review provides an overview of the recent progress in various aspects of TR prevention. Different strategies for

Dr. R. D. McKerracher, Dr. J. Guzman-Guemez, Prof. R. G. A. Wills, Prof. S. M. Sharkh
Faculty of Engineering & the Environment
University of Southampton
Southampton SO17 1BJ, UK
E-mail: R.D.McKerracher@soton.ac.uk

Prof. D. Kramer
Faculty of Mechanical Engineering
Helmut-Schmidt University
Holstenhofweg 85, 22043 Hamburg, Germany

 The ORCID identification number(s) for the author(s) of this article can be found under <https://doi.org/10.1002/aesr.202000059>.

© 2021 The Authors. Advanced Energy and Sustainability Research published by Wiley-VCH GmbH. This is an open access article under the terms of the Creative Commons Attribution License, which permits use, distribution and reproduction in any medium, provided the original work is properly cited.

DOI: 10.1002/aesr.202000059

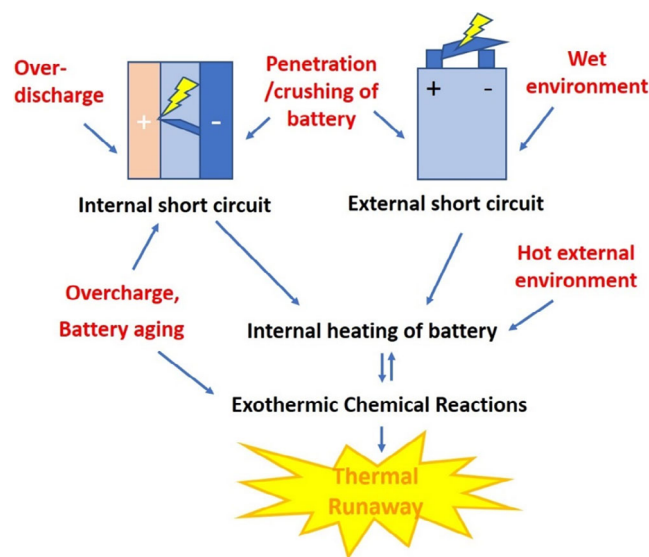


Figure 1. Diagram showing the sequences of events leading to TR.

avoiding and mitigating TR are compared, including developments within the past couple of years. Promising innovations that keep pace with the recent evolution of lithium-ion technology are identified.

2. Mechanism of TR

TR of a lithium-ion cell can be caused by several events which lead to uncontrolled heating (Figure 1). Internal short circuits may be caused by a crushing or piercing event or cell abuse such as overcharging (causing lithium plating at anode) or overdischarging (causing copper plating at the cathode). The same events may lead to an external short circuit when the battery terminals contact each other. It has also been known for a release of water into the battery to cause an external short circuit.^[9] The recommended SAE and ISO safety tests for lithium-ion batteries attempt to induce these root causes of TR via the following abuse scenarios: controlled crushing, penetration, drop, vibration, rolling, immersion in water, mechanical shock, simulated fuel fire, high-temperature storage, extremely cold environment, rapid charge/discharge, thermal shock, overcharge, overdischarge, and short circuit.^[7,8,10] These tests provide data on how each cell will behave outside normal operating conditions.

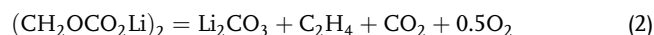
Of all abuse conditions, overcharging is particularly likely to lead to TR because more energy is being continuously added to the cell, even as the heat inside reaches dangerous levels. Overcharging leads to deposition of lithium-metal onto the surface of the fully lithiated anode, which can then react exothermically with the solid-electrolyte interface (SEI), and at the cathode side, the electrolyte will be oxidized as the safe voltage window is exceeded.^[11] The voltage safety window depends on the chemistry of the battery, for example, a lithium-ion battery with LiFePO₄ cathode and graphite anode has a maximum charge voltage of 3.65 V and a minimum discharge voltage of 2.5 V, but with a LiCoO₂ cathode, the maximum charging voltage is 4.2 V and the minimum discharge voltage is 3.0 V.

Regardless of the initial root cause of TR (Figure 1), a certain sequence of events will occur following an increased temperature inside the cell. Once the cell temperature exceeds the maximum safe operating temperature, the cell enters the heat-temperature-reaction (HTR) loop, which is a self-accelerating process where heat causes exothermic chemical reactions, leading to further heating, which leads to a chain of further reactions.^[12] The end result of the HTR loop is TR, with an exponential increase in temperature.^[13] The exothermic decomposition reactions are governed by Arrhenius reaction kinetics.

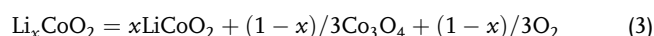
$$Q(T) = Q_0 \exp(-E_a/RT) \quad (1)$$

where $Q(T)$ is the heat transferred at a given temperature (T), E_a is the activation energy, R is the universal gas constant, and Q_0 is the pre-exponential constant.^[14] These kinetics can be used in models which predict the pathway of TR.^[15,16]

The first step of the HTR loop is decomposition of the SEI, which produces ethene (C₂H₄) and CO or CO₂, causing swelling of the cell, for example^[17]



The SEI decomposition has an onset temperature of 80 °C^[18] but some reports suggest it may even begin at a lower temperature.^[19,20] The SEI decomposition temperature is lowered as the state of charge (SOC) decreases.^[21] As exothermic decomposition of the SEI causes a further increase in temperature; eventually at 100–120 °C, the electrolyte will decompose and/or the separator will begin to melt, generating CO₂, CO, and a mixture of hydrocarbon gases depending on cell chemistry.^[18] An internal short circuit is now highly likely. During a short circuit, as much as 70% of the cell energy can be released in less than 1 min, causing the temperature to increase further.^[22] Above 130 °C, the cathode begins to break down, a process which generates oxygen, for example^[17]



This is the step that makes the cell highly flammable. Above 150 °C, this reaction can become self-sustaining if the heat cannot be dissipated away quickly enough, and the cell is now fully in TR (Figure 2) with an exponentially increasing temperature (Figure 3).^[23] As gases build up exponentially from the cathode decomposition (Figure 3), they will vent or explode out of the cell,

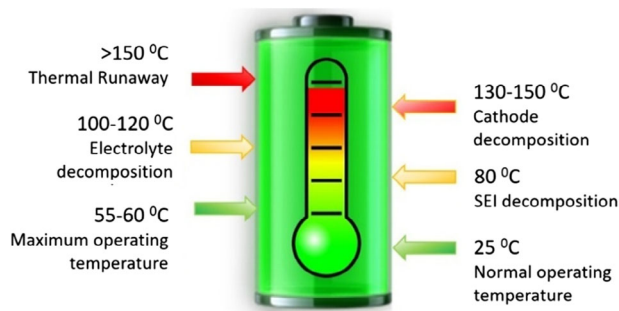


Figure 2. Schematic diagram showing the stages leading toward TR.

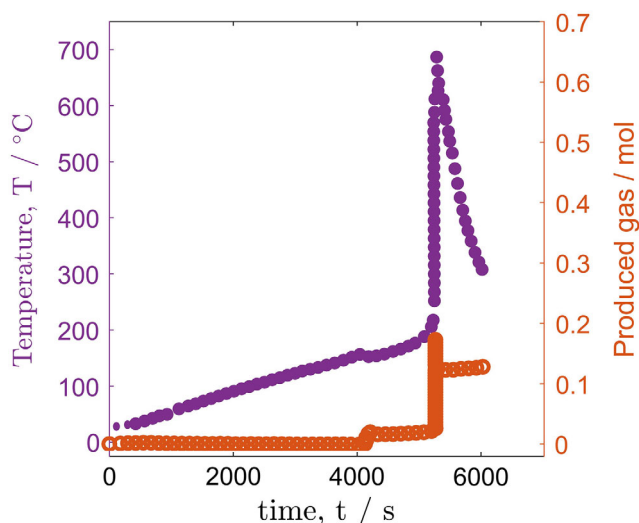


Figure 3. Accelerated rate calorimetry of a lithium-ion cell in TR. There are two events that cause the emission of a gas: a) electrolyte decomposition and b) cathode decomposition.^[24]

and the highly flammable mixture can be easily ignited by an electrical spark. As the temperature increases further, eventually, all cell materials, including the anode and cell casing, will decompose. The cell temperature can approach 900 °C during this step.^[24]

Even more seriously, a domino effect may then ensue where the cell in TR triggers neighboring cells in the battery pack to go into TR.^[18] The propagation of TR between cells accelerates if this process is not stopped and moves along the pathway of lowest thermal resistance.^[25] Propagation from the cells in the center of the pack is most likely because there are more heat-transfer paths to neighboring cells. For this reason, it is very important to isolate a cell from others in the battery pack once it begins to go into TR, via thermal insulation and cooling and by breaking the electrical contacts to the cell. The next section of this Review looks at each of the methods that have been used to prevent TR and chain reactions between cells.

3. Techniques Deployed to Prevent TR

Systems used to prevent TR are either external, managing external temperature, and electrically isolating a cell or internal, preventing the heat-generating processes inside the cell. Internal systems often add less volume but may be more expensive to implement. Some systems are more effective than others, and more than one prevention system can be used at the same time to increase safety.^[26] The following sections examine external methods: (thermal management systems [3.1] and BMSs [3.2]) and internal methods (cell-level mechanisms [3.3]).

3.1. Thermal Management Systems

The principle behind thermal management systems is simple: to maintain the cells within their safe temperature limits during periods of operation and standby. There are two components

of a thermal management system: 1) the coolant which is actively circulated or passively fixed around the cell to prevent TR during charging and 2) layers of heat-dissipating/-insulating/fire-retardant materials wrapped around cells which prevent TR from spreading to other cells and causing fire. In the case of active thermal management systems, the components and circuitry are a subsystem of the BMS which will be covered in the next section.

In part (ii) of the thermal management system, thermally conductive graphite sheets are often used for heat dissipation,^[27,28] and polyimides or polyester films make excellent thin fire-retardant materials.^[29] A recent innovation in insulation is nanosilicon balloon insulator (NASBIS), which is very thin and flexible. Its thermal conductivity is lower than air at 0.02 W mK⁻¹.^[30] The downside of using all these safety-enhancing layers is that the extra materials take up volume and decrease energy density, reducing the range of electric vehicles.

The choice of part (i), the cell coolant, is not straightforward, and the features of each method are discussed in the following section.

3.1.1. Cell Coolants

To cool the battery, active methods such as fans and refrigerants or passive methods such as heat sinks or heat shields are used. In practice, a combination of these methods may be used (Figure 4).^[31–33] Recent research has focused on delivering systems which are more compact and have higher heat conductivity and capacity. Circulating liquid coolant rather than air improves both heat conductivity and capacity and leads to greater uniformity of temperature throughout the battery pack.^[34] However, this comes at the cost of adding volume and extra mechanical parts to the cell (Figure 4c). Liquid coolants remain the popular choice for Tesla in its electric vehicles because they are the most effective for batteries operating at high charging rates.^[35]

The parts for a refrigerant system (Figure 4a) are also more compact than a liquid system (Figure 4c), but refrigerants have the disadvantage of adversely cooling the cell during winter. A different option is to use a phase-change material (PCM)-based cooling system, which has no need for these extra components and occupies a smaller volume (Figure 4b). Some of the coolants used in electric vehicles are shown in Table 1.

PCMs absorb heat from cells by undergoing a phase change, which requires a large amount of latent heat. They have been shown to prevent TR if used in sufficient quantities.^[25] Many different PCMs have been proposed, from simple materials such as paraffin wax in electric scooter batteries^[36,37] to more complex materials such as eutectic salts.^[10,38] It is difficult to directly compare PCMs as they have been tested with batteries with different chemistries under different conditions; however, there are certain advantages and disadvantages associated with each type (Table 2); for example, metallic salts such as sodium thiosulfate pentahydrate have the lowest cost in terms of \$/kW but may undergo sedimentation over time and degrade in quality.^[39] The thermal conductivity of hydrocarbons such as paraffin is so poor that they have to be mixed with a conductive agent such as expanded graphite, and the composite may degrade over time due to melting. Eutectic salts and fatty acids do not undergo

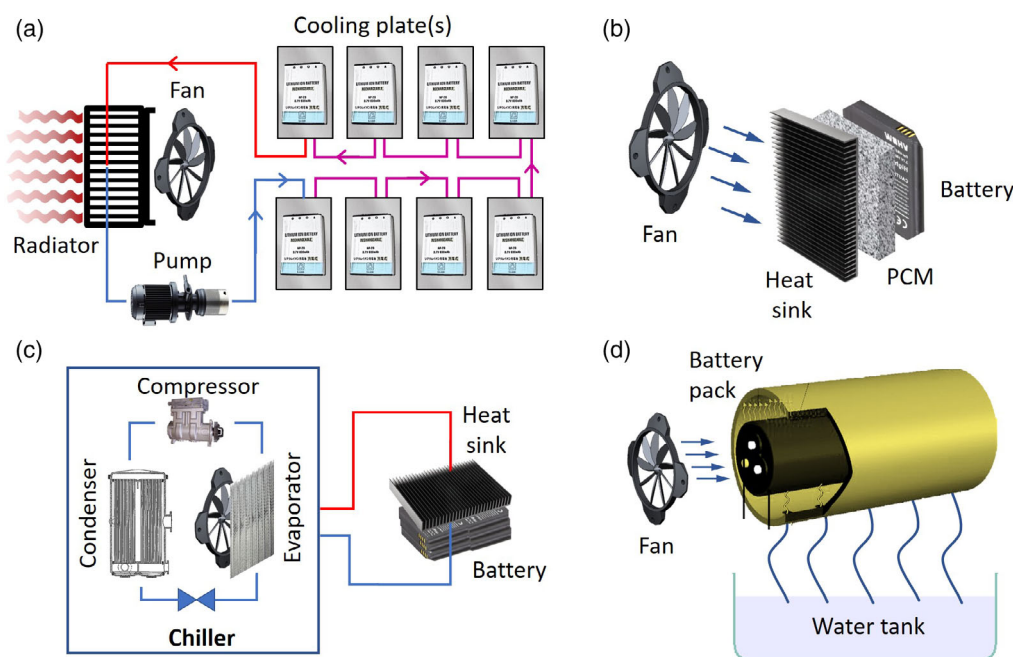


Figure 4. Schematic diagram of thermal management systems for lithium-ion batteries: a) refrigerant cooling with cooling plates,^[31] b) PCM with fan,^[32] c) liquid coolant circulated in a chiller,^[32] and d) mist cooling with an evaporating liquid.^[33]

Table 1. Examples of different types of thermal management used in commercial lithium-ion batteries.

Coolant	Type	Specific heat capacity [kJ kg K ⁻¹]	Comments	Applications	Ref.
Air	Gas	1.0	Less effective at high C rates but lowest cost	Nissan Leaf	[122]
				Ford C-max hybrid	
Water/glycol	Liquid	3.4	Increased weight and complexity	Tesla vehicles	[123]
Paraffin wax	PCM	1.77	Poor thermal conductivity, needs conductive additive	Electric Scooters	[36]
Tetra-fluoropropene	Refrigerant	0.7	Lower volume	BMW i3	[124]
Not ideal in winter due to low temperature					

Table 2. Examples of PCMs used in lithium-ion batteries.

Material	Phase change	Specific heat capacity [kJ kg K ⁻¹] ^{a)}	Thermal conductivity [W Mk ⁻¹] ^{a)}	Comments	Ref.
Graphite/paraffin composite	Solid–liquid	2.5	7.9 0.21 without graphite ^[125]	Hybrid with air cooling.	[26]
Palmitic acid	Dehydration	1.9	0.16	Nontoxic, compact	[39]
Sodium thiosulfate pentahydrate	Dehydration	1.9	0.56	Sedimentation after phase change	[39]
MgCl ₂ (H ₂ O) ₆	Eutectic melt	1.6	0.93	Compact, more expensive	[126]

^{a)}Values are given for the initial phase before change.

phase separation but may be more expensive than hydrocarbons such as paraffin.^[39]

Since 2015, a new development to improve the effectiveness of solid PCMs with low thermal conductivity has been to add heat pipes made of very high thermal conductivity material such as

copper to conduct latent heat from the PCM toward the outside of the battery pack.^[40,41] For example, a sandwich structure consisting of the battery, a plate of PCM–graphite composite, and a copper plate can be created, with the copper plate attached to a copper heat pipe with a radiating fin to remove heat efficiently

from the battery pack.^[42] The surface temperature of a battery surrounded by a PCM with copper heat pipes remained below 32 °C during three charge–discharge cycles. An identical system without heat pipes reached 45 °C by the end of the third charging cycle, highlighting the effectiveness of adding a heat pipe to the system.^[42]

Finally, another recent idea for a new kind of phase-change cooling system is to immerse the cells in a pool of evaporating liquid, known as mist cooling (Figure 4d).^[43] This model is still under development and is complex to operate but has the potential to achieve a very uniform temperature inside the battery pack.^[39] The system has the dual advantage of fluid convection to remove heat, combined with the latent heat energy of the liquid–gas phase change. The liquid used has to have a boiling point close to the cell operating temperature such as Novec 7000 hydrofluoroether^[44] or water vapor.^[43]

In summary, thermal management systems with coolant are an effective way to keep the temperature of lithium-ion batteries low and prevent TR, but compromises have to be struck between cost, volume of coolant, and heat capacity/conductivity of the coolant. Thermal management systems do not prevent the root causes of TR, and failure of the cooling system can cause the lithium-ion cells to overheat. It is also important to note that extreme events such as cell rupture and short circuit may cause a release of energy beyond which the cooling system can mitigate.^[45] Therefore, it is crucial to constantly monitor the state of health of the cells in the battery pack using a BMS. This is discussed in the following section.

3.2. Battery Management Systems

The BMS is an electronic system which monitors the state of the cells inside the battery, calculates secondary data, and uses this information to control the balance of the charge, discharge, and temperatures of the cells.^[46] The BMS detects when the battery pack is degraded or abused and manages the risks using mitigation measures (e.g., electrically isolating or inhibiting one or multiple cells). The BMS is completely stable when it keeps the system within the safe operating area (SOA). If one or more batteries reaches TR, the BMS may become unstable (Figure 5). The design of the BMS, including operating voltage, maximum current, and volume, is specific to the application, with requirements being different for automotive versus stationary batteries. BMS are available off the shelf for common applications, and several commercial modules can be connected via a controller area network bus to manage any number of cells. Devices that

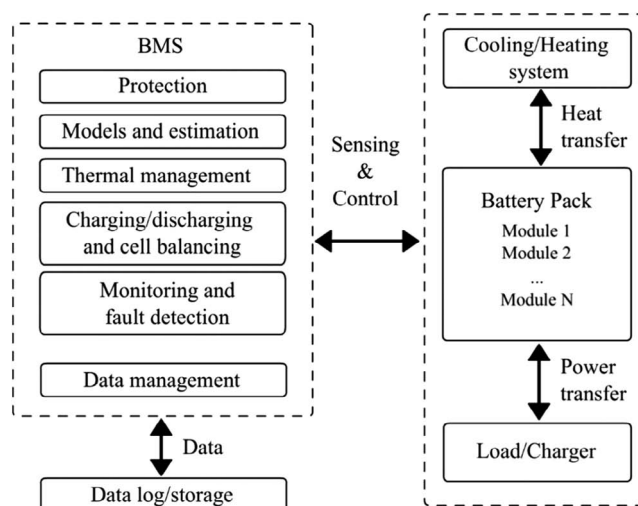


Figure 6. Schematic diagram of typical BMS functions and interfaces, based on the study by Barreras et al.^[120]

have unusual demands (e.g., healthcare devices with high safety needs) will need a BMS with bespoke design.

A basic BMS will monitor the cell voltages, conduct protection functions against over-voltage, high current, high temperature, and provide passive balancing. The second generation of BMSs is modular rather than centralized and can actively balance the battery pack based on cell-to-cell-level measurements, which allow a higher degree of control and protection.^[47,48] Figure 6 shows a typical BMS system, with listed subsystems including cell balancing, charging, and discharging control, fault monitoring, and detection, mitigation, and active thermal management (see Section 3.1).^[48] The subsystems of the BMS are described in the following sections.

3.2.1. Cell Balancing

Cell equalization (balancing the voltages in the cell) is essential as it ensures uniform charging of the battery to maximize the energy delivered and increase battery lifetime.^[49] Due to different initial conditions (e.g., inconsistent manufacturing) and different operating conditions (power distribution, internal and external temperatures, or position in the battery pack), batteries will have different internal parameters and uneven performance. However, the manufacturer's datasheets provide reasonable limits on the battery SOA in terms of power and temperatures, so the BMS can be calibrated to work within these parameters.

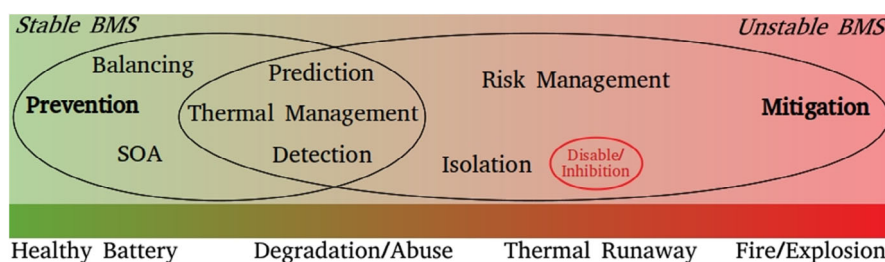


Figure 5. Processes of the BMS relative to the battery health.

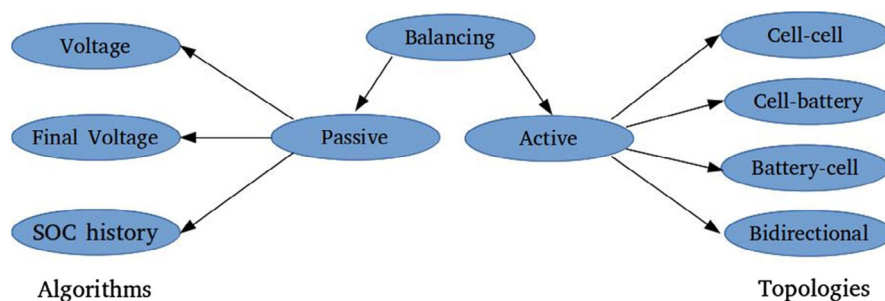


Figure 7. Types of balancing in a BMS.^[50]

There are two types of battery balancing: passive balancing, where energy from the most charged cell is dissipated away as heat via resistive balancers, and active balancing, where energy is drawn from the most charged cell and redistributed to the other cells via converters. As shown in **Figure 7**, passive balancing is algorithm dependent, using voltage, final voltage, or SOC history data. Voltage balancing assumes that a specific voltage corresponds to a specific SOC for any given cell. Final voltage balancing uses the voltage at the end of the charging cycle to calculate SOC. In both cases the terminal voltage is often measured instead of the open-circuit voltage (OCV). The OCV can be deduced if the impedance including internal resistance, charge-transfer resistance, and Warburg elements of each cell is known; however, the resistances change over time. This means that cells with higher resistances instead of those with the highest SOC will be discharged, increasing the imbalance in SOC. This problem can be overcome by SOC balancing using algorithms based on SOC history, which increases the effectiveness of balancing hardware by ≈ 3.7 times.^[50] However, this uses significant computing power and complexity to store the SOC of each cell, calculate the difference in charge of each cell compared with the least charged cell, and apply the corresponding balancing current for each cell in the next charge/discharge cycle to make the SOC of all cells even.^[50]

Active balancing is topology dependent, using power electronic converters or a transistor configuration to enable energy transfer in any of the four ways: cell to cell, cell to battery, battery to cell, and bidirectional (**Figure 7**). It is claimed that cell to cell is the most efficient, using around 90% of the overall energy.^[50] As active balancing requires one or more converters (which produce heat), further energy is required to travel and the less efficient the system becomes. In most cases, wasted energy is more for active than passive balancers,^[51] and active balancing is only recommended for applications where passive balancing would be difficult.^[50] Examples are large packs with mismatched cells, fast-charging batteries, or cells that always operate at high temperatures. Active balancing is also more expensive, and research aims to reduce costs: a reduced-component balancer proposed for a 20 kWh battery pack promises to decrease the cost by 37% compared with a typical active balancer.^[49]

3.2.2. TR Detection Methods

In addition to balancing voltage and SOC, a BMS has to detect the onset of TR. Most simply, this can be done by measuring the

temperature of the battery cells. One of the main challenges is the difficulty of measuring the temperature of individual cells and acquiring their internal (core) temperature. This would allow earlier measures to be taken before damage or TR occurs, as the increase in temperature occurs internally before it increases externally. A noninvasive method has been proposed, which uses energy conservation equations to determine the core temperature of a cylindrical cell from its outside surface temperature distribution.^[52] The results (**Figure 8a**) showed close agreement with a battery with an actual set of thermocouples inside. Another publication developed models to produce estimations of temperature distribution throughout the battery in real time utilizing a Kalman filter and a tuned thermal model with finite temperature sensors.^[53] However, so far, most models of TR are based on the surface temperature of the cell which can be directly measured.

Studies of the evolution of the battery surface temperature (**Figure 8b**) show that there are different stages.^[54,55] The SEI decomposition starts at T_1 , and the melting process of the separator begins at T_2 (usually 130–160 °C). Above this temperature, the separator loses its mechanical integrity and starts to induce internal micro-short circuits. The point T_3 is the TR trigger (or critical) temperature, which initiates an exponential increase in temperature caused by the exothermic reactions and short circuits. This temperature is usually under 200 °C,^[54,55] but this will depend on battery chemistry,^[51] as well as SOC,^[56] thermal transport within the cell, thermal transport from the cell surface to the outside, and the cell geometry.^[57] Temperatures under T_1 are within the safe operating area, and temperatures under T_3 can potentially be considered “reversible” areas, although the severity of the damage inside the cell increases with increasing temperature. It has been observed that T_1 increases and T_3 decreases as the cell ages.^[58] A combination of experimental work with modeling^[53,55,59] concluded that T_2 is critical for evaluating battery safety, because a cell with higher T_2 will be more likely to pass abuse tests, such as oven heating, nail penetration, or other mechanical abuse.^[60,61]

Measurements other than temperature could be used by the BMS to detect the state of health of a battery cell. For example, in situ impedance characterization in real time observed that the Warburg element of cell impedance was particularly sensitive to increased operation temperature.^[58] Impedance measurements of charge-transfer resistance are emerging as a low-cost method for the BMS to monitor the state of health of cells during use.^[62]

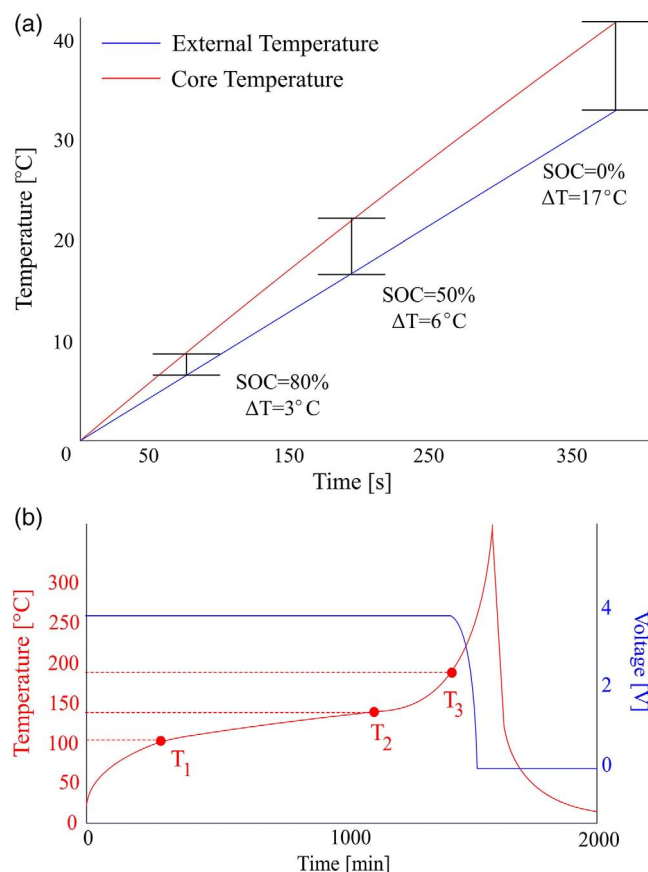


Figure 8. a) Theoretical relationship between the external and core temperature of a cell.^[52] b) External temperature and voltage of a battery cell.^[54]

Some of the newer BMSs use incremental capacity analysis to assess the battery state of health. If the state of health is defined by the maximum capacity of the cell as a percentage of the original maximum capacity, then capacity readings should give an idea of state of health with each cycle. However, batteries are rarely fully discharged, with vehicles usually operated at 40–80% depth of discharge.^[63] The BMS can use algorithms to calculate the state of health from standard sensor inputs (voltage, current, and temperature) in real time. These algorithms are based on the derivative of the partial charging curve with respect to the cell voltage.^[63,64] Compared with other computational methods of estimating capacity in real time, such as Kalman filter-based algorithms and machine learning, relatively small amounts of experimental data and computational power are required.^[65]

Noninvasive analysis methods can also be used to detect specific battery failure events from the battery voltage reading over time. For example, weakened contacts in the electrical circuitry surrounding the battery can be detected by statistical comparison with an equivalent circuit model,^[66] and lithium plating at the anode can be inferred by identifying a characteristic stripping plateau at the discharging plateau of the battery.^[67]

Another approach to TR detection by the BMS is to detect gas release. An increase in temperature and gassing both increase pressure inside the cell, and gas sensors can be used in tandem with volume expansion measurements (via pressure sensors) of

cells to detect gas evolution in the earliest stage of TR (SEI decomposition).^[68] The exact quantity and composition of gas evolved during decomposition of the SEI depend on cell chemistry, but because of unavoidable impurities, lithium carbonates are present at the cathode SEI and residual water at the anode SEI; this means that all lithium-ion batteries will generate CO_2 and H_2 in measurable concentrations.^[24,69] Evaporated electrolyte can also be detected by sensors for volatile organic compounds.^[70] Results of implementing a gas sensor into a lithium-ion battery system^[71] show that the sensors can detect electrolyte leaks and an increase in volatile organic compound concentration and can detect battery failures earlier than the temperature sensors. However, it is still unclear if this is always effective as success varies according to sensor position and sensitivity, mechanical restrictions in the battery system, and decomposition onset temperature. Ideally, the sensors would detect the gases at ppm levels, but in practice, this is challenging.^[72]

3.2.3. TR Mitigation by the BMS

If the battery pack ceases to operate within the SOA, and TR has been detected, and mitigation measures are necessary. These measures can be implemented at a materials level, cell level, or system (battery pack) level.^[73] The BMS has control over mitigation at cell and system level. Mitigation methods used by the BMS can include system shut down (either the whole battery pack or one subsection) via safety switches, which trip in the event of increased current or temperature, deploying the thermal management system, releasing inert gas to quench flames, opening vents to remove heat and gases, and closing vents to prevent escape of fire.^[73,74]

Some of the mitigating methods deployed by the BMS are shown in Figure 9. At cell level, the topology of the BMS could electrically isolate all of the cell(s) that approach TR. Alternatively, at system level, the battery or pack could be prematurely discharged by the BMS to decrease risk. As TR becomes more advanced, a successive string of mitigation measures will have to be applied, becoming increasingly extreme and fast acting. While the cells are still in the safe operating area, the BMS can balance the cells and deploy the active thermal management system (fans or coolant pumps) to prevent increased temperature. If one cell leaves the SOA, the BMS can shut off all cells connected in series in that part of the battery and redistribute charge. The BMS can control the release of inert gases to trap and dilute the battery vent gases to prevent fire.^[75] If TR persists and spreads, total system shutdown is crucial, as well as rapid sealing of vents if fire is detected.^[74] The battery should be surrounded by caged structures, which contain an explosion, and the cell casing should be made of nonflammable materials, with similar materials between cells to prevent TR propagation.^[73]

3.3. Cell-Level Mechanisms to Avoid TR

To address TR at a deeper level, mechanisms can be built into the structure of the cell as a preventative measure. The components can be modified to reduce the likelihood of short circuits, to shut down the cell at elevated temperatures, and to prevent the release of volatile gases. The following sections discuss these innovations in detail.

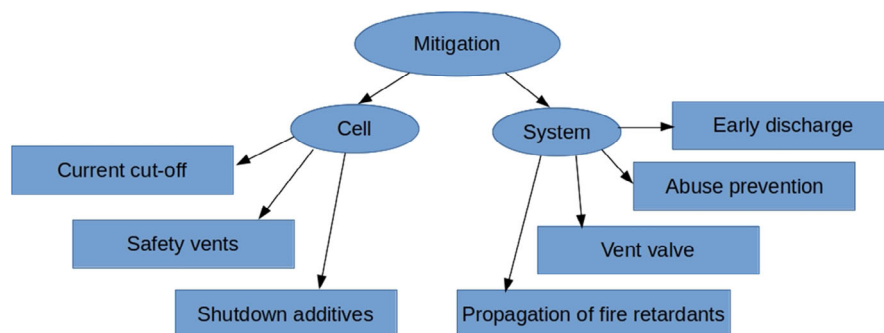


Figure 9. Some mitigation methods at cell and system level.

3.3.1. Electrode Modifications

The first aspect of electrode design to consider is to avoid geometries which increase the likelihood of lithium plating, which can lead to an internal short circuit.^[76] It is important to avoid inhomogeneity in the particle distribution and sharp edges. The active surface of a lithium-ion battery anode is always cut slightly larger in area than the cathode to avoid lithium-ion dendrite formation at the edge.^[77]

The chemistry of the electrodes and the SEI is crucial to cell stability and how likely the cells are to undergo TR. The most stable cathode material in current use is LiFePO₄ (LFP), which is stable up to 310 °C.^[78,79] Other commonly used cathode materials, such as layered lithiated metal oxides, generate a large amount of oxygen on heating.^[80] The anode will also decompose as the temperature increases further, and it has been found through differential scanning calorimetry that a Li₄Ti₅O₁₂ anode is more thermally stable than graphite.^[80] The newer, high-capacity anodes made from Si and Sn are still under investigation, and they face unique challenges due to their higher energy density and extreme volume expansion when lithiated.^[81]

Figure 10 shows accelerated rate calorimetry of four different cell chemistries; below 200 °C, it is notable that the cell with the LFP cathode has the lowest rate of temperature increase (ΔT) compared with other cell chemistries. The two cells with NMC cathodes release a much larger amount of heat energy before cell shutdown, especially the cell with NMC442 cell with Li(Ni_{0.4}Co_{0.2}Mn_{0.4})O₂-graphite chemistry (Figure 10). The reason for the enhanced stability of LFP cathodes is believed to be the strong phosphorous-oxygen bonds, which inhibit release of O₂ from the cathode upon heating.^[82] LFP also produces the lowest volume of gas during TR.^[24]

In addition to the chemistry, the capacity of the cell strongly affects the energy released during TR. An accelerated calorimetry study of LCO-graphite cells with 33, 1000, and 3300 mAh capacities showed that the energy released during TR is in proportion to the capacity of the cell; the 33 mAh cell underwent incomplete TR.^[83] The authors suggest that this is due to the larger proportion of inactive materials blended with the cathode materials in the lower-capacity cell, which absorbs the heat produced. Although it is impractical for automotive applications to use low-capacity cells with a large amount of “wasted” volume, this may be useful information for applications where volume is not at a premium, as the results of this research suggest that

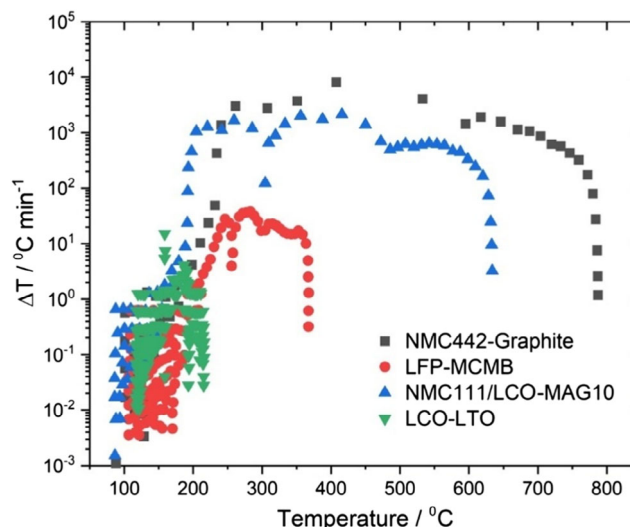


Figure 10. Accelerated calorimetry of lithium-ion cells with four different cell chemistries. NMC442 = Li(Ni_{0.4}Co_{0.2}Mn_{0.4})O₂, LFP = LiFePO₄, MCMB = mesocarbon microbeads, NMC111 = Li(NiCoMn)_{1/3}O₂, LCO = LiCoO₂, MAG10 = Cu-graphite, and LTO = Li₄Ti₅O₁₂.^[121]

larger banks of lower-capacity cells would be at a negligible risk of undergoing TR.

Aside from the discussion on electrode materials, it has been indicated that as TR begins at the SEI, the electrolyte is the most crucial part of the cell to initiate the TR process.^[80] Recent discoveries of thermally stable electrolytes are discussed in the next section.

3.3.2. Electrolyte Composition

As TR begins at the SEI, the electrolyte composition is an important part of preventing TR. The first generation of lithium-ion battery electrolytes is made by dissolving a salt, such as LiPF₆ or LiClO₄, in a mixture of ethylene carbonate with diethyl carbonate. This mixture becomes unstable above 4.5 V, so although it works for LiCoO₂-graphite, LiFePO₄-graphite, and other well-established chemistries, for the next generation of lithium-ion batteries (e.g., LNMO-graphite) which have to endure higher voltages and fast charging currents, these electrolytes will need improvement for their safety.^[84] Organic fluorocompounds are

currently under development to allow formation of a more stable SEI that is resistant to high voltages.^[84]

The electrolyte can also be manufactured with flame-retardant properties^[85–88] to stop mixtures of gases from igniting, at the cost of increasing electrolyte volume with complex additives such as cyclophosphazenes.^[85] However, more fundamentally, the electrolyte can be designed to be nonliquid, to prevent the release of flammable gases, which progresses TR. Certain polymer electrolytes, either gel or solid, are used in this respect but suffer lower ionic conductivities.^[89] Solid polymer electrolytes may be flammable,^[90] so must be specifically designed with noncombustible materials, but solid ceramics are inherently safe in this regard. In 2020, a fire-retardant, self-healing polymer electrolyte was reported, which can reform via a network of hydrogen bonds when cut.^[91]

Another less common solution is to use a completely nonflammable inorganic electrolyte such as an aqueous solution.^[92–95] However, aqueous lithium-ion batteries have many limitations, mainly the much lower voltage and energy densities and difficulty in preventing the oxygen reduction reaction. The problem of oxygen reduction may decrease by use of water-in-salt electrolyte, which is an extremely concentrated salt solution.^[96–98] Research published in 2020 suggests that this is achievable and with a cell voltage of 2.7 V.^[92] Further work is needed to develop the technology and ensure long-term stability. A recent discovery of nature-derived aqueous carboxymethyl cellulose gels with self-healing properties is an interesting new avenue.^[99,100]

Table 3 shows some of the emerging flame-retardant battery technologies. Those with nonflammable liquid organic electrolytes offer performance characteristics that are more like existing lithium-ion batteries. Until recently aqueous lithium-ion batteries lagged far behind in terms of their voltage and energy density but the latest research into water-in-salt electrolytes with halide lithium electrodes has yielded exceptional results with a cell voltage of 4.7 V and a specific energy of 304 Wh kg^{−1}, considering the mass of the full cell.^[101] This large specific energy is achieved due to formation of a (LiBr)_{0.5}–(LiCl)_{0.5}–C intercalation compound, which can intercalate roughly one lithium ion per four carbon atoms. Solid polymer and solid-state batteries have comparably high voltages but typically suffer from low power densities due to the poor ionic conductivity of solids compared with

liquids. However, a novel hybrid system published in 2020 combined materials from ionic liquids and polymers in a nonflammable hybrid system, which reached a power density of 476 W kg^{−1}. This is competitive with liquid systems while conferring some of the advantages of solid state (increased mechanical strength and resistance to short circuits).

An innovative approach to high-safety lithium-ion batteries is to render the cell highly resistive during storage and reactivate it on demand using internal self-heating via a nickel metal sheet. This property is achieved using triallyl phosphate (TAP) molecules which polymerize at the SEI at room temperature.^[102] This reduces problems such as cell aging and self-discharge, leading to improved battery state of health. The passivated cells are completely resistant to the causes of TR. However, to be used, the battery must be subjected to controlled heating to 60 °C for 10–20 s to decrease the charge-transfer resistance of the SEI before use, so a cell chemistry that is stable at these temperatures is required. The authors did not supply a mechanism for how this decrease in resistance works, but it may be due to increased mobility of conductive polymer chains. It is important to note that while active, the cells are not completely immune from TR, and the operating temperature of 60 °C edges toward the temperature at which the SEI may begin to decompose. However, the authors explained that the addition of TAP prevents some of the destructive reactions that occur at the SEI, which is why it is successful at preventing TR.

3.3.3. Separator Design

The separator can also play a role in decreasing the conductivity of the cell as the temperature increases. A commonly used polymer is polyethylene blended with other polymers for mechanical strength. Poly(ethylene) has a melting temperature of 130 °C, so the cell will be rendered inoperable above this temperature as the electronic pathways are broken by melting.^[103] Unfortunately, this is not reversible, so the cell will then have to be broken down for recycling. Also, this thermal shutdown separator is limited by the time it takes for the polymer to melt, which may not be sufficient if the rate of heat generation is very high.

Research on improved thermal shutdown separators has recently focused on polyacrylonitrile (PAN), which does not melt

Table 3. Recent flame-resistant lithium-ion batteries in the literature.

Battery Cathode/Anode ^{a)}	Electrolyte ^{b)}	Type	Avg. cell voltage [V]	Specific energy [Wh kg ^{−1}]	Specific power [W kg ^{−1}]	Ref.
LiNi _{0.5} Mn _{1.5} O ₄ /graphite	TFEP	Liquid organic	4.6	–	–	[127]
NCM622/graphite	LiPF ₆ /EC/EMC Triallyl phosphate	Liquid organic	3.7	166	440	[102]
LiMn ₂ O ₄ /Al ₂ O ₃ @LiTiTi ₂ (PO ₄) ₃	LiTFSI/H ₂ O	Aqueous	2.6	170	300	[92]
(LiBr) _{0.5} –(LiCl) _{0.5} /Graphite	LiTFSI/LiOTf/H ₂ O	Aqueous	4.2	304	336	[101]
LiFePO ₄ /Li	PEO/LiTFSI	Solid polymer	3.45	–	–	[90]
LiCo ₂ /Li	LATP	Solid State	4.0	600	60	[128]
LiFePO ₄ /Li	LiTFSI, LLZO, PP13TFSI IL, in PVDF-HFP matrix	Hybrid Solid–ionic liquid	3.4	–	476	[129]

^{a)}NCM = nickel cobalt manganese oxide; ^{b)}TPEP = 2-(2,2,2-trifluoroethoxy)-1,3,2-dioxaphospholane 2-oxide; EC = ethylene carbonate; EMC = ethylene methyl carbonate; LiTFSI = lithium bis(trifluoromethanesulfonyl)imide; LiOTf = lithium trifluoromethane sulfonate; LATP = lithium aluminum titanium phosphate; LLZO = lithium lanthanum zirconium oxide; PP13TFSI = N-methyl-N-propylpiperidinium bis(trifluoromethanesulfonyl)imide.

until 322 °C, but undergoes a reversible thermal expansion above 80 °C, causing a tenfold increase in resistance over a 10 °C temperature increase.^[104] The PAN can be electrospun as a composite with PVdF to improve its wettability by the electrolyte.^[105]

Composites of polymers and ceramics, such as TiO₂-PVdF and CaCO₃-PTFE, are another promising avenue of research.^[106] The ceramic ensures that the separator maintains its mechanical integrity and makes the cell more tolerant of abuse, whereas the polymer undergoes a structural change as the temperature increases, blocking the pores and rendering the cell nonconductive.

Aside from causing thermal shutdown, separators can also be designed with chemical or mechanical properties to prevent formation of lithium dendrites at the anode. Some ceramic separators developed for other lithium-containing batteries such as Li-metal and Li-S may be of interest. One such separator is vermiculite, a hydrated laminar ceramic with high strength and Young's modulus, which is resistant to penetration by lithium-metal dendrites.^[107] Another recent innovation is the coating of a polymer separator with a TiO₂ layer on the cathode side that reacts with and destroys any lithium dendrites that have penetrated the separator.^[108] A similar separator which consumes lithium has also been made by sandwiching silica nanoparticles in between separator layers.^[109]

A publication in 2018 reported a unique ceramic separator made from a renewable resource, eggshell membranes,^[110] which was shown to be effective in preventing the formation of lithium dendrites after long-term cycling at the 5.0 C rate compared with a commercial Celgard membrane. The safety and sustainability of this material made it an attractive candidate for future lithium-ion battery separators compared with traditional petrochemical materials. It has been estimated that 400 kWh of energy is needed to produce a 1 kWh lithium-ion battery, producing around 75 kg of CO₂ emissions;^[111] the use of nature-derived materials could decrease some of these emissions.

3.3.4. Temperature-Sensitive Additives (Positive Temperature Coefficient [PTC] Materials)

Certain ferroelectric semiconductors have a positive temperature coefficient (PTC) relationship between resistivity and temperature and become dramatically less conductive above their Curie temperature,^[112] the point at which there is an abrupt change in the crystal structure of the material. This means that

if these materials are used as the conductive additive in lithium-ion battery electrodes, the cell conductivity could undergo a several orders of magnitude decrease above a certain temperature. The great challenge is to find a material with a Curie temperature close to room temperature; most materials have a temperature well above 200 °C.

The class of materials used in ceramic PTC resistors has the general formula Ba_{1-x}LnTiO₃, where Ln is a metal from the lanthanide series. For example, recently Ba_{0.7}Sr_{0.3}TiO₃ and Ba_{0.9}Sr_{0.1}TiO₃ ceramics displayed Curie temperatures of 38 and 54 °C, respectively, which are only just below the onset temperature of TR.^[113] Ceramic PTC materials are only semiconducting (the conductivity of BaTiO₃ is close to 10⁻⁷ S cm⁻¹ at room temperature)^[114] so require the addition of a conductive additive (Table 4).

Apart from conductive additives, the polymer binders inside the cell can also be designed as temperature sensitive, ideally beginning at temperatures below 100 °C. For example, LiCoO₂ sandwiched with poly(methyl methacrylate) mixed with Super P carbon black was found to have PTC properties, increasing resistance at 80–120 °C such that the cell capacity of 140 mAh.g⁻¹ decreases to 8.4 mAh.g⁻¹ at 110 °C, blocking transfer of most of the current through the cell.^[115] Carbon/polyethylene composites are another PTC material;^[116] the challenge is to improve the contact between the conductive particles embedded in the polymer matrix.

The most successful strategy for safety is to deploy PTC materials at the SEI as a protective layer, rather than generally mixing them with the cathode materials. A composite of poly(3-decylthiophene) spray coated onto an LCO cathode showed a strong PTC effect, with electronic conductivity decreasing from around 10⁻³ Scm⁻¹ at room temperature to 10⁻⁶ Scm⁻¹ at 80–100 °C, the ideal range for preventing TR.^[117] However, adding the PTC materials as a separate layer comes with the disadvantages of adding bulk to the cathode, and also decreasing the conductivity at the SEI, as carbon-polymer composites are not especially conductive. A publication from 2019 used the conductive polymer poly(3-octylpyrrole)/carbon as a PTC material directly mixed into the LCO cathode material and showed increased resistivity by four orders of magnitude from room temperature to 120 °C. The 30.3 Scm⁻¹ conductivity of the cathode at room temperature compares favorably with the 4 Scm⁻¹ conductivity of Super P carbon.^[118] Another strategy to increase conductivity is to use nickel nanoparticles in the polymer composite, which are much

Table 4. Properties of recent PTC materials for lithium-ion batteries. RT = room temperature.

Material	PTC Temp range [°C]	RT conductivity	Order of magnitude decrease in conductivity/increase in resistivity	Refs.
Poly(3-octylpyrrole)/C	120	30.3 Scm ⁻¹	4	[118]
Poly(3-dodecylthiophene)	90–100	–	4	[130]
Polyethylene microspheres	110	0.3 mScm ⁻¹	Not measured	[131]
Poly(3-ethylenedioxythiophene) (PEDOT/C)	100–120	600 Scm ⁻¹	>4	[132]
PVDF/Ni nanoparticles	75–170	300 Scm ⁻¹	8	[119]
BaTiO ₃ -Bi _{0.5} Li _{0.5} TiO ₃	100–160	≈10 ⁻⁷ Scm ⁻¹	3.5	[133]
Ba _{1-x} LnTiO ₃	54–100	≈10 ⁻⁷ Scm ⁻¹	2–4	[113]
Bi _{1/2} Ti _{1/2} O ₃ doped BaTiO ₃	125–200	≈10 ⁻⁷ Scm ⁻¹	7–8	[134]

more conductive than carbon, leading to a 300 Scm^{-1} conductivity of the composite film at room temperature.^[119] A practical feature of these PVdF/Ni films is that the temperature range of the PTC response can be tuned by altering the polymer/Ni ratio.

At the time of writing, research into polymer additives is more numerous than ceramic materials, because the number of polymer-carbon composites exhibiting PTC behavior in the appropriate temperature range is significantly greater. Care needs to be taken that the PTC materials are nonflammable and are compatible with the other materials in the battery so that there will be no unwanted side reactions.

4. Summary and Conclusion

The prevention of TR in lithium-ion batteries can be addressed using many different methods: functions of BMSs, devices which dissipate heat, and internal modifications of the cells which inhibit the chemical reactions that lead to TR. There have been numerous recent innovations in all these areas. The development of PTC materials and other thermal shutdown materials that reversibly enter a low-conductivity state above 60°C is highlighted as being of particular importance, as they can improve safety by tackling the root causes of TR (Figure 1). This material engineering at the cell level should be the focus of future research, aimed at making a cell in which TR is not possible. This will reduce the size, cost, and complexity of the higher layers of battery safety protection (Figure 11), such as the insulating materials, thermal, and BMSs. These layers (numbers 4–6 in Figure 11) will still be required to balance cell voltages and act as a failsafe, but they will be supported by underlying protection from the cell materials (numbers 1–3 in Figure 11).

The appropriate technology for the battery pack depends on the intended application. For example, in automotive batteries,

power density is high, and the consequences of TR can be most tragic, giving an incentive to use as many layers of protection against TR as possible. However, there is limited volume inside the vehicle. Designing the layers of protection against TR will need to be a compromise between battery performance (i.e., maximum power/capacity), space saving, and cost. Here, the use of novel self-healing polymer electrolytes and hybrid liquid–solid-state electrolytes may be of great interest, as they have shown improved safety without compromising performance and adding bulk. The higher layers of protection including the BMS and coolant will need to be compact and efficient in their use of energy. Mist cooling is a promising new technology to achieve a highly uniform temperature without the need for pumps to circulate a coolant. To decrease the need for mitigation functions on the BMS, early TR detection systems have to be enhanced. A BMS which can model the internal temperature of the cell from real-time data and prevent the cell reaching a critical temperature is an essential area for further research.

In addition to concerns with safety, the impact of lithium-ion batteries on the environment should be at the forefront of researchers' minds when introducing new innovations to a battery. Nature-derived materials, such as the dendrite-preventing separators manufactured from eggshell membranes (Section 3.3.3), are an example of how lithium-ion batteries could be made using more sustainable production methods. The other parts of the battery, including the PCMs, insulation, BMS, and cooling system, should be designed for efficient use of materials and energy.

Acknowledgements

The authors acknowledge funding from the EPSRC under the title "ISCF Wave 1: Improved lifetime performance and safety of electrochemical energy stores through functionalization of passive materials and components," grant reference EP/R021295/1.

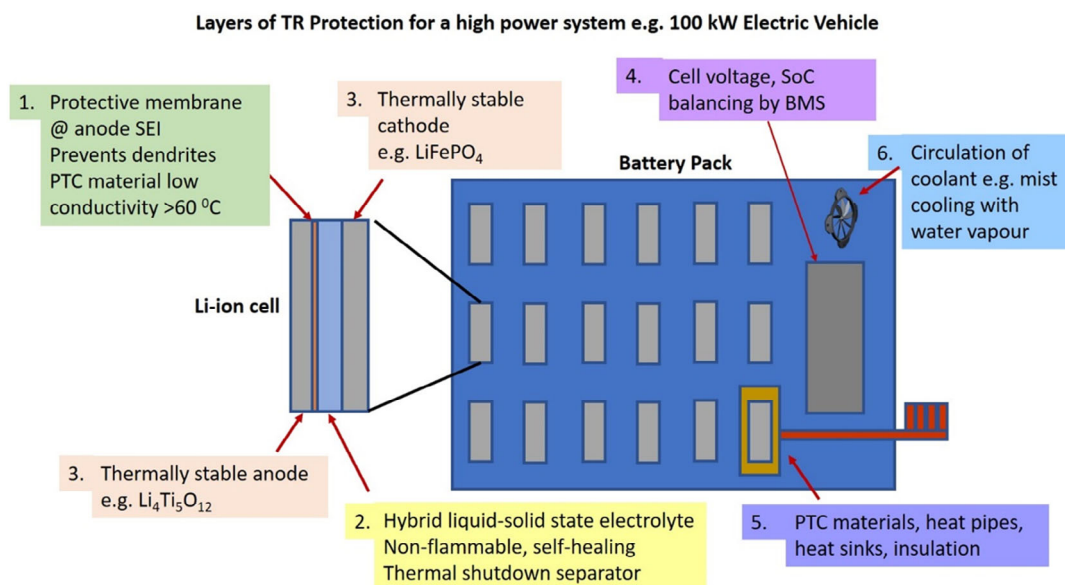


Figure 11. Layers of protection against TR in a high-power lithium-ion battery. The layers are ordered to how close they are to the internal protection of the cell.

Conflict of Interest

The authors declare no conflict of interest.

Keywords

battery management, lithium-ion batteries, positive thermal coefficient materials, thermal runaway

Received: October 29, 2020

Revised: February 11, 2021

Published online:

- [1] Battery Requirements for Future Automotive Applications, European Council for Automotive R&D, <https://eucar.be/wp-content/uploads/2019/08/20190710-EG-BEV-FCEV-Battery-requirements-FINAL.pdf> (accessed: February 2021).
- [2] F. Shi, H. Yu, X. Chen, T. Cui, H. Zhao, X. Shi, in *Lecture Notes in Electrical Engineering*, Springer Verlag, Dordrecht **2019**, pp. 1–11.
- [3] D. Ouyang, M. Chen, Q. Huang, J. Weng, Z. Wang, J. Wang, *Appl. Sci.* **2019**, 9, 2483.
- [4] E. A. Kapp, D. S. Wroth, J. T. Chapin, *Transp. Res. Rec. J. Transp. Res. Board* **2020**, 2674, 584.
- [5] Recommendations on the Transport of Dangerous Goods Manual of Tests and Criteria, United Nations Publication, https://unece.org/fileadmin/DAM/trans/danger/publi/manual/Rev7/Manual_Rev7_E.pdf (accessed: February 2021).
- [6] L. Bravo Diaz, X. He, Z. Hu, F. Restuccia, M. Marinescu, J. V. Barreras, Y. Patel, G. Offer, G. Rein, *J. Electrochem. Soc.* **2020**, 167, 090559.
- [7] D. H. Doughty, C. C. Crafts, *FreedomCAR Electrical Energy Storage System Abuse Test Manual for Electric and Hybrid Electric Vehicle Applications*, Technical Report, Sandia National Laboratories **2006**.
- [8] J2464: Electric and Hybrid Electric Vehicle Rechargeable Energy Storage System (RESS) Safety and Abuse Testing – SAE International, https://www.sae.org/standards/content/j2464_200911/ (accessed: February 2021).
- [9] C. Xu, M. Ouyang, L. Lu, X. Liu, S. Wang, X. Feng, *ECS Trans.* **2017**, 77, 209.
- [10] H. Nazir, M. Batool, F. J. Bolivar Osorio, M. Isaza-Ruiz, X. Xu, K. Vignarooban, P. Phelan, Inamuddin, A. M. Kannan, *Int. J. Heat Mass Transf.* **2019**, 129, 491.
- [11] D. Ren, X. Feng, L. Lu, X. He, M. Ouyang, *Appl. Energy* **2019**, 250, 323.
- [12] D. Ren, H. Hsu, R. Li, X. Feng, D. Guo, X. Han, L. Lu, X. He, S. Gao, J. Hou, Y. Li, Y. Wang, M. Ouyang, *eTransportation* **2019**, 2, 100034.
- [13] N. E. Galushkin, N. N. Yazvinskaya, D. N. Galushkin, *J. Electrochem. Soc.* **2018**, 165, A1303.
- [14] K. Shah, A. Jain, *Int. J. Energy Res.* **2019**, 43, 1827.
- [15] Md Said, Mohd Tohir, *Processes* **2019**, 7, 703.
- [16] H. Chen, J. E. H. Buston, J. Gill, D. Howard, R. C. E. Williams, E. Read, A. Abaza, B. Cooper, J. X. Wen, *J. Electrochem. Soc.* **2021**, 168, 010502.
- [17] X. Feng, M. Ouyang, X. Liu, L. Lu, Y. Xia, X. He, *Energy Storage Mater.* **2018**, 10, 246.
- [18] J. T. Warner, in *Lithium-Ion Battery Chemistries*, Elsevier, Amsterdam **2019**, pp. 43–77.
- [19] T. Yoon, M. S. Milien, B. S. Parimalam, B. L. Lucht, *Chem. Mater.* **2017**, 29, 3237.
- [20] Q. Wang, J. Sun, X. Yao, C. Chen, *Thermochim. Acta* **2005**, 437, 12.
- [21] A. Pfrang, A. Kriston, V. Ruiz, N. Lebedeva, F. di Persio, in *Emerging Nanotechnologies in Rechargeable Energy Storage Systems*, Elsevier Inc., Amsterdam **2017**, pp. 253–290.
- [22] H. Maleki, J. N. Howard, *J. Power Sources* **2009**, 191, 568.
- [23] J. W. Dold, *Q. J. Mech. Appl. Math.* **1985**, 38, 361.
- [24] A. W. Golubkov, D. Fuchs, J. Wagner, H. Wilsche, C. Stangl, G. Fauler, G. Voitic, A. Thaler, V. Hacker, *RSC Adv.* **2014**, 4, 3633.
- [25] Z. Y. Jiang, Z. G. Qu, J. F. Zhang, Z. H. Rao, *Appl. Energy* **2020**, 268, 115007.
- [26] Z. Ling, F. Wang, X. Fang, X. Gao, Z. Zhang, *Appl. Energy* **2015**, 148, 403.
- [27] K. M. Kim, Y. S. Jeong, I. C. Bang, *Eng. Sci. Technol. an Int. J.* **2019**, 22, 610.
- [28] P. Sun, Z. Gong, Z. Chen, in *Proc. – 2019 12th Int. Conf. Intelligent Computation Technology and Automation ICICTA 2019*, Institute of Electrical and Electronics Engineers Inc., Piscataway, NJ **2019**, pp. 724–729.
- [29] J. Shi, Y. Xia, Z. Yuan, H. Hu, X. Li, H. Zhang, Z. Liu, *Sci. Rep.* **2015**, 5, 1.
- [30] NASBIS Thermal Management | Panasonic Industrial Devices, <https://na.industrial.panasonic.com/whats-new/thermal-management-solution-nasbis> (accessed: October 2020).
- [31] S. Yang, C. Ling, Y. Fan, Y. Yang, X. Tan, H. Dong, *Int. J. Electrochem. Sci.* **2019**, 14, 6077.
- [32] Q. Wang, B. Jiang, B. Li, Y. Yan, *Renewable Sustainable Energy Rev.* **2016**, 64, 106.
- [33] G. Fang, Y. Huang, W. Yuan, Y. Yang, Y. Tang, W. Ju, F. Chu, Z. Zhao, *RSC Adv.* **2019**, 9, 9951.
- [34] M. Al-Zareer, I. Dincer, M. A. Rosen, *Appl. Therm. Eng.* **2020**, 165, 114378.
- [35] A. Tomaszewska, Z. Chu, X. Feng, S. O'Kane, X. Liu, J. Chen, C. Ji, E. Endler, R. Li, L. Liu, Y. Li, S. Zheng, S. Vetterlein, M. Gao, J. Du, M. Parkes, M. Ouyang, M. Marinescu, G. Offer, B. Wu, *eTransportation* **2019**, 1, 100011.
- [36] S. A. Khateeb, S. Amiruddin, M. Farid, J. R. Selman, S. Al-Hallaj, *J. Power Sources* **2005**, 142, 345.
- [37] S. A. Khateeb, M. M. Farid, J. R. Selman, S. Al-Hallaj, *J. Power Sources* **2004**, 128, 292.
- [38] K. Y. Leong, M. R. Abdul Rahman, B. A. Gurunathan, *J. Energy Storage* **2019**, 21, 18.
- [39] S. Landini, J. Leworthy, T. S. O'Donovan, *J. Energy Storage* **2019**, 25, 100887.
- [40] Y. Ye, Y. Shi, L. H. Saw, A. A. O. Tay, *Int. J. Heat Mass Transf.* **2016**, 92, 893.
- [41] Y. Ye, L. H. Saw, Y. Shi, A. A. O. Tay, *Appl. Therm. Eng.* **2015**, 86, 281.
- [42] Z. Y. Jiang, Z. G. Qu, *Appl. Energy* **2019**, 242, 378.
- [43] L. H. Saw, H. M. Poon, H. S. Thiam, Z. Cai, W. T. Chong, N. A. Pambudi, Y. J. King, *Appl. Energy* **2018**, 223, 146.
- [44] S. Rashidi, F. Hormozi, M. M. Sarafraz, *J. Therm. Anal. Calorim.* **2020**, 143, 1815.
- [45] L. Lao, Y. Su, Q. Zhang, S. Wu, *J. Electrochem. Soc.* **2020**, 167, 090519.
- [46] ARTECH HOUSE USA : Battery Power Management for Portable Devices, <https://us.artechhouse.com/Battery-Power-Management-for-Portable-Devices-P1583.aspx> (accessed: February 2021).
- [47] T. Stuart, F. Fang, X. Wang, C. Ashtiani, A. Pesaran, in *SAE Technical Paper*, SAE International, Warrendale, PA **2002**.
- [48] S. S. Madani, M. J. Swierczynski, S. K. Kaer, in *2017 12th Int. Conf. Ecological Vehicles and Renewable Energies, EVER 2017*, Institute of Electrical and Electronics Engineers Inc., Piscataway, NJ **2017**.
- [49] P. A. Cassani, S. S. Williamson, in *Conf. Proc. – IEEE Applied Power Electronics Conf. Expo. – APEC, IEEE, Piscataway, NJ* **2009**, pp. 465–471.
- [50] D. Andrea, *Battery Management Systems for Large Lithium Ion Battery Packs*, Artech House, Boston, MA **2010**.
- [51] A. Kelkar, Y. Dasari, S. S. Williamson, in *2020 IEEE Int. Conf. Power Electronics Smart Grid Renewable Energy, PESGRE 2020*, Institute Of Electrical And Electronics Engineers Inc., Piscataway, NJ **2020**.

- [52] D. Anthony, D. Wong, D. Wetz, A. Jain, *Int. J. Heat Mass Transf.* **2017**, 111, 223.
- [53] Y. Xiao, *IEEE Trans. Ind. Electron.* **2015**, 62, 3112.
- [54] S. Abada, M. Petit, A. Lecocq, G. Marlaire, V. Sauvart-Moynot, F. Huet, *J. Power Sources* **2018**, 399, 264.
- [55] X. Feng, S. Zheng, D. Ren, X. He, L. Wang, H. Cui, X. Liu, C. Jin, F. Zhang, C. Xu, H. Hsu, S. Gao, T. Chen, Y. Li, T. Wang, H. Wang, M. Li, M. Ouyang, *Appl. Energy* **2019**, 246, 53.
- [56] P. Huang, C. Yao, B. Mao, Q. Wang, J. Sun, Z. Bai, *Energy* **2020**, 213, 119082.
- [57] I. Esho, K. Shah, A. Jain, *Appl. Therm. Eng.* **2018**, 145, 287.
- [58] F. Leng, C. M. Tan, M. Pecht, *Sci. Rep.* **2015**, 5, 12967.
- [59] D. Ren, X. Liu, X. Feng, L. Lu, M. Ouyang, J. Li, X. He, *Appl. Energy* **2018**, 228, 633.
- [60] H. Wang, E. Lara-Curzio, E. T. Rule, C. S. Winchester, *J. Power Sources* **2017**, 342, 913.
- [61] F. Leng, C. M. Tan, M. Pecht, *Sci. Rep.* **2015**, 5, 12967.
- [62] D. A. Howey, V. Yufit, P. D. Mitcheson, G. J. Offer, N. P. Brandon, in *2013 World Electric Vehicle Symp. and Exhibition, EVS 2014*, Institute of Electrical and Electronics Engineers Inc., Piscataway, NJ **2014**.
- [63] E. Riviere, A. Sari, P. Venet, F. Meniere, Y. Bultel, *Batteries* **2019**, 5, 37.
- [64] C. Weng, Y. Cui, J. Sun, H. Peng, *J. Power Sources* **2013**, 235, 36.
- [65] L. Zheng, J. Zhu, D. D. C. Lu, G. Wang, T. He, *Energy* **2018**, 150, 759.
- [66] M. Ma, Y. Wang, Q. Duan, T. Wu, J. Sun, Q. Wang, *Energy* **2018**, 164, 745.
- [67] M. Petzl, M. A. Danzer, *J. Power Sources* **2014**, 254, 80.
- [68] B. Rowden, N. Garcia-Araez, in *Energy Reports*, Elsevier Ltd, Amsterdam **2020**, pp. 10–18.
- [69] N. E. Galushkin, N. N. Yazvinskaya, D. N. Galushkin, *J. Electrochem. Soc.* **2019**, 166, A897.
- [70] Y. Pan, X. Feng, L. Lu, M. Ouyang, *ECS Meet. Abstr.* **2019**, MA2019-01, 590.
- [71] M. Wenger, R. Waller, V. R. H. Lorentz, M. Marz, M. Herold, in *IECON Proc., Industrial Electronics Conf.*, Institute of Electrical and Electronics Engineers Inc., Piscataway, NJ **2014**, pp. 5654–5659.
- [72] D. Sturk, L. Rosell, P. Blomqvist, A. Ahlberg Tidblad, *Batteries* **2019**, 5, 61.
- [73] X. Feng, D. Ren, X. He, M. Ouyang, *Joule* **2020**, 4, 743.
- [74] S. Purushothaman, in *2019 IEEE Industry Applications Society Annual Meeting IAS 2019*, Institute of Electrical and Electronics Engineers Inc., Piscataway, NJ **2019**.
- [75] W. Li, H. Wang, Y. Zhang, M. Ouyang, *J. Energy Storage* **2019**, 24, 100775.
- [76] S. Santhanagopalan, G.-H. Kim, M. Keyers, A. A. Pesaran, K. Smith, J. Neubauer, *Design and Analysis of Large Lithium-Ion Battery Systems*, Artech House, Boston, MA **2015**.
- [77] B. Son, M. H. Ryou, J. Choi, S. H. Kim, J. M. Ko, Y. M. Lee, *J. Power Sources* **2013**, 243, 641.
- [78] F. Gao, H. Liu, K. Yang, C. T. Zeng, S. Wang, M. Fan, H. Wang, *Int. J. Electrochem. Sci.* **2020**, 15, 1391.
- [79] B. Lei, W. Zhao, C. Ziebert, N. Uhlmann, M. Rohde, H. Seifert, *Batteries* **2017**, 3, 14.
- [80] A. Kvascha, C. Gutiérrez, U. Osa, I. de Meatza, J. A. Blazquez, H. Macicior, I. Urdampilleta, *Energy* **2018**, 159, 547.
- [81] X. Liu, D. Ren, H. Hsu, X. Feng, G. L. Xu, M. Zhuang, H. Gao, L. Lu, X. Han, Z. Chu, J. Li, X. He, K. Amine, M. Ouyang, *Joule* **2018**, 2, 2047.
- [82] P. J. Bugryniec, J. N. Davidson, S. F. Brown, in *Energy Procedia*, Elsevier Ltd, Amsterdam **2018**, pp. 74–78.
- [83] K. Son, S. M. Hwang, S. G. Woo, J. K. Koo, M. Paik, E. H. Song, Y. J. Kim, *J. Ind. Eng. Chem.* **2020**, 83, 247.
- [84] Q. Li, J. Chen, L. Fan, X. Kong, Y. Lu, *Green Energy Environ.* **2016**, 1, 18.
- [85] T. Dagger, B. R. Rad, F. M. Schappacher, M. Winter, *Energy Technol.* **2018**, 6, 2011.
- [86] L. Jiang, Q. Wang, K. Li, P. Ping, L. Jiang, J. Sun, *Sustain. Energy Fuels* **2018**, 2, 1323.
- [87] K. Liu, Y. Liu, D. Lin, A. Pei, Y. Cui, *Sci. Adv.* **2018**, 4, eaas9820.
- [88] S. Chen, J. Zheng, L. Yu, X. Ren, M. H. Engelhard, C. Niu, H. Lee, W. Xu, J. Xiao, J. Liu, J. G. Zhang, *Joule* **2018**, 2, 1548.
- [89] J. Allen, in *Energy Reports*, Elsevier Ltd, Amsterdam **2020**, pp. 217–224.
- [90] Y. Cui, J. Wan, Y. Ye, K. Liu, L. Y. Chou, Y. Cui, *Nano Lett.* **2020**, 20, 1686.
- [91] B. Zhou, M. Yang, C. Zuo, G. Chen, D. He, X. Zhou, C. Liu, X. Xie, Z. Xue, *ACS Macro Lett.* **2020**, 9, 525.
- [92] L. Chen, L. Cao, X. Ji, S. Hou, Q. Li, J. Chen, C. Yang, N. Eidson, C. Wang, *Nat. Commun.* **2020**, 11, 1.
- [93] J. Y. Luo, W. J. Cui, P. He, Y. Y. Xia, *Nat. Chem.* **2010**, 2, 760.
- [94] D. Bin, Y. Wen, Y. Wang, Y. Xia, *J. Energy Chem.* **2018**, 27, 1521.
- [95] A. S. Lakhnot, T. Gupta, Y. Singh, P. Hundekar, R. Jain, F. Han, N. Koratkar, *Energy Storage Mater.* **2020**, 27, 506.
- [96] L. Chen, L. Cao, X. Ji, S. Hou, Q. Li, J. Chen, C. Yang, N. Eidson, C. Wang, *Nat. Commun.* **2020**, 11, 1.
- [97] L. Suo, O. Borodin, T. Gao, M. Olguin, J. Ho, X. Fan, C. Luo, C. Wang, K. Xu, *Science* **2015**, 350, 938.
- [98] W. Sun, L. Suo, F. Wang, N. Eidson, C. Yang, F. Han, Z. Ma, T. Gao, M. Zhu, C. Wang, *Electrochem. commun.* **2017**, 82, 71.
- [99] J. Liu, H. Yuan, X. Tao, Y. Liang, S. J. Yang, J. Huang, T. Yuan, M. Titirici, Q. Zhang, *EcoMat* **2020**, 2, e12019.
- [100] Y. Zhao, Y. Zhang, H. Sun, X. Dong, J. Cao, L. Wang, Y. Xu, J. Ren, Y. Hwang, I. H. Son, X. Huang, Y. Wang, H. Peng, *Angew. Chemie – Int. Ed.* **2016**, 55, 14384.
- [101] C. Yang, J. Chen, X. Ji, T. P. Pollard, X. Lü, C. J. Sun, S. Hou, Q. Liu, C. Liu, T. Qing, Y. Wang, O. Borodin, Y. Ren, K. Xu, C. Wang, *Nature* **2019**, 569, 245.
- [102] S. Ge, Y. Leng, T. Liu, R. S. Longchamps, X. G. Yang, Y. Gao, D. Wang, D. Wang, C. Y. Wang, *Sci. Adv.* **2020**, 6, 7633.
- [103] J. Allen, in *Energy Reports*, Elsevier Ltd, Amsterdam **2020**.
- [104] Y. Huai, J. Gao, Z. Deng, J. Suo, *Ionics (Kiel)*. **2010**, 16, 603.
- [105] Z. Liang, Y. Zhao, Y. Li, *Energies* **2019**, 12, 3391.
- [106] C. J. Orendorff, *Electrochem. Soc. Interface* **2012**, 21, 61.
- [107] R. Xu, Y. Sun, Y. Wang, J. Huang, Q. Zhang, *Chinese Chem. Lett.* **2017**, 28, 2235.
- [108] S. S. Zhang, X. Fan, C. Wang, *J. Mater. Chem. A* **2018**, 6, 10755.
- [109] K. Liu, Y. Liu, D. Lin, A. Pei, Y. Cui, *Sci. Adv.* **2018**, 4, eaas9820.
- [110] L. Ma, R. Chen, Y. Hu, W. Zhang, G. Zhu, P. Zhao, T. Chen, C. Wang, W. Yan, Y. Wang, L. Wang, Z. Tie, J. Liu, Z. Jin, *Energy Storage Mater.* **2018**, 14, 258.
- [111] D. Larcher, J. M. Tarascon, *Nat. Chem.* **2015**, 7, 19.
- [112] J. Kudrnovsky, G. Bouzerar, I. Turek, *Appl. Phys. Lett.* **2007**, 91, 102509.
- [113] A. Yu, Q. Li, *Ceram. Int.* **2020**, 46, 8796.
- [114] T. Amirah, T. Sulong, R. Aina, M. Osman, M. S. Idris, Z. Azhar, Z. Jamal, *EPJ Web Conf.* **2017**, 162, 01050.
- [115] X. Lan, Z. Limin, H. Zhang, A. I. Xinping, *Chin. Sci. Bull.* **2012**, 57, 4205.
- [116] L. Wen, J. Liang, J. Chen, Z. Chu, H. Cheng, F. Li, *Small Methods* **2019**, 3, 1900323.
- [117] L. Xia, S. L. Li, X. P. Ai, H. X. Yang, Y. L. Cao, *Energy Environ. Sci.* **2011**, 4, 2845.
- [118] H. Li, F. Wang, C. Zhang, W. Ji, J. Qian, Y. Cao, H. Yang, X. Ai, *Energy Storage Mater.* **2019**, 17, 275.
- [119] M. Li, Y. Shi, H. Gao, Z. Chen, *Adv. Funct. Mater.* **2020**, 30, 1910328.
- [120] J. V. Barreras, C. Fleischer, A. E. Christensen, M. Swierczynski, E. Schaltz, S. J. Andreasen, D. U. Sauer, *IEEE Trans. Ind. Appl.* **2016**, 52, 5086.
- [121] S. Zheng, L. Wang, X. Feng, X. He, *J. Power Sources* **2018**, 378, 527.

- [122] A. A. Franco, *Rechargeable Lithium Batteries: From Fundamentals to Applications*, Elsevier Inc., Amsterdam **2015**.
- [123] A. J. Martyr, M. A. Plint, *Engine Testing*, Elsevier Ltd, Amsterdam **2007**.
- [124] (PDF) Plotting of P-H and T-S diagrams of fluoropropylenes, https://www.researchgate.net/publication/273573808_Plotting_of_P-H_and_T-S_diagrams_of_fluoropropylenes (accessed: October 2020).
- [125] A. Agarwal, R. M. Sarviya, in *Materials Today: Proc.*, Elsevier Ltd, Amsterdam **2017**, pp. 779–789.
- [126] J. Pereira da Cunha, P. Eames, *Appl. Energy* **2016**, 177, 227.
- [127] Q. Zheng, Y. Yamada, R. Shang, S. Ko, Y. Y. Lee, K. Kim, E. Nakamura, A. Yamada, *Nat. Energy* **2020**, 5, 291.
- [128] Z. Kou, C. Miao, P. Mei, Y. Zhang, X. Yan, Y. Jiang, W. Xiao, *Ceram. Int.* **2020**, 46, 9629.
- [129] X. Zhou, H. Jiang, H. Zheng, Y. Sun, X. Liang, H. Xiang, *J. Membr. Sci.* **2020**, 603, 117820.
- [130] H. Li, X. Zhang, C. Zhang, Y. Cao, H. Yang, X. Ai, F. Zhong, *Energy Technol.* **2020**, 8, 2000365.
- [131] C. Zhang, H. Li, S. Wang, Y. Cao, H. Yang, X. Ai, F. Zhong, *J. Energy Chem.* **2020**, 44, 33.
- [132] G. Shi, X. Cai, W. Wang, G. Wang, *Macromol. Chem. Phys.* **2020**, 221, 2000144.
- [133] M. Yang, Z. Peng, C. Wang, X. Fu, *Ceram. Int.* **2016**, 42, 17792.
- [134] W. Huo, Y. Qu, *Sensors Actuators, A* **2006**, 128, 265.



Rachel McKerracher graduated with an M.Chem. from Oxford University in 2009 and completed her Ph.D. at the University of Southampton in 2012. She is currently a postdoctoral researcher in the Energy Technology Research Group at the University of Southampton. She has worked on several battery systems including metal–air, aluminum–ion, and lithium–ion systems, and her latest research is focused on improving sustainability in battery design and materials.



Jorge Guzman-Guemez graduated from the Instituto Politécnico Nacional, Mexico City, in 2013, before completing his Ph.D. at the University of Southampton in 2018. He is currently a postdoctoral researcher at the University of Southampton. His expertise lies in the fields of power systems analysis, control theory, and FPGA programming.



Suleiman Sharkh is professor of Power Electronics, Machines and Drives in the Faculty of Engineering and the Physical Sciences at the University of Southampton. He is the Deputy Director of the Southampton EPSRC “Energy Storage and its Applications” Centre for Doctoral Training. He has supervised over 20 Ph.D. students. His inventions and research have contributed to commercial products including tidal turbine generators, novel electric motors, gas compressors and grid connected invertors.